HAL
open science

Response of intertidal benthic microalgal biofilms to a coupled light-temperature stress: evidence for latitudinal adaptation along the Atlantic coast of Southern Europe.

Martin Laviale, Alexandre Barnett, João Ezequiel, Bernard Lepetit, Silja Frankenbach, Vona Méléder, João Serôdio, Johann Lavaud

To cite this version:

Martin Laviale, Alexandre Barnett, João Ezequiel, Bernard Lepetit, Silja Frankenbach, et al.. Response of intertidal benthic microalgal biofilms to a coupled light-temperature stress: evidence for latitudinal adaptation along the Atlantic coast of Southern Europe.. Environmental Microbiology, Society for Applied Microbiology and Wiley-Blackwell, 2015, pp.3662-3677. 10.1111/1462-2920.12728 . hal-01097838

HAL Id: hal-01097838

https://hal.archives-ouvertes.fr/hal-01097838

Submitted on 9 Jan 2015

HAL is a multi-disciplinary open access archive for the deposit and dissemination of scientific research documents, whether they are published or not. The documents may come from teaching and research institutions in France or abroad, or from public or private research centers.

L'archive ouverte pluridisciplinaire **HAL**, est destinée au dépôt et à la diffusion de documents scientifiques de niveau recherche, publiés ou non, émanant des établissements d'enseignement et de recherche français ou étrangers, des laboratoires publics ou privés.

Response of intertidal benthic microalgal biofilms to a coupled light-temperature stress: evidence for latitudinal adaptation along the Atlantic coast of Southern Europe.

Martin Laviale,[1*] Alexandre Barnett,[2] João Ezequiel,[1] Bernard Lepetit,[2#] Silja Frankenbach,[1] Vona Méléder,[2,3] João Serôdio[1] and Johann Lavaud[2]

[1] Departamento de Biologia and CESAM – Centro de Estudos do Ambiente e do Mar, Universidade de Aveiro, Campus de Santiago, 3810-193 Aveiro, Portugal

[2] UMRi7266 LIENSs 'Littoral, Environnement et Sociétés', CNRS/Université de La Rochelle, Institut du Littoral et de l'Environnement, 2 rue Olympe de Gouges, 17000 La Rochelle, France.

[3] LUNAM Université, Université de Nantes, EA 21 60 MMS 'Mer, Molécules, Santé', 2 rue de la Houssinière, BP 92 208, 44322, Nantes Cedex 3, France

Current address: Plant Ecophysiology, Department of Biology, University of Konstanz, Universitätsstraße 10, 78457 Konstanz, Germany

* Corresponding author:

Departamento de Biologia and CESAM – Centro de Estudos do Ambiente e do Mar, Universidade de Aveiro, Campus de Santiago, 3810-193 Aveiro, Portugal

Phone: +351 234 370 968; Fax: +351 234 372 587; E-mail: martin.laviale.bio@gmail.com

Running title: microphytobenthos response to light-temperature stress

Summary:

Although estuarine microphytobenthos (MPB) is frequently exposed to excessive light and temperature conditions, little is known on their interactive effects on MPB primary productivity. Laboratory and *in situ* experiments were combined to investigate the short-term joint effects of high light (HL) and high temperature (37°C *vs*. 27°C) on the operating efficiency of photoprotective processes (vertical migration *vs.* non-photochemical quenching: NPQ) exhibited by natural benthic diatom communities from two intertidal flats in France (FR) and Portugal (PT). A clear latitudinal pattern was observed, with PT biofilms being more resistant to HL stress, regardless the effect of temperature, and displaying a lower relative contribution of vertical migration to photoprotection and a stronger NPQ *in situ*. However, higher temperature leads to comparable effects, with photoinhibition increasing to about 3-times (i.e. from 3 to 10 % and from 8 to 22 % in PT and FR sites, respectively). By using a number of methodological novelties in MPB research (lipid peroxidation quantification, Lhcx proteins immunodetection), this study brings a physiological basis to the previously reported depression of MPB photosynthetic productivity in summer. They emphasize the joint role of temperature and light in limiting, at least transiently (i.e. during emersion), MPB photosynthetic activity *in situ*.

Introduction

Estuarine tidal flats are one of the most productive ecosystems on Earth, largely owing to the photosynthetic productivity of benthic microalgae communities, or microphytobenthos (MPB) (Underwood and Kromkamp, 1999). MPB communities are often dominated by motile pennate diatoms (Haubois *et al.*, 2005; Méléder *et al.*, 2007; Ribeiro *et al.*, 2013). In fine sediment habitats, they undergo rhythmic vertical migration patterns in the upper layers of the sediment following tidal/dial cycles (Saburova and Polikarpov, 2003; Consalvey *et al.*, 2004; Coelho *et al.*, 2011). During daylight emersion, the upward migration of cells results in the formation of transient photosynthetic biofilms which are thus periodically exposed to variable and extreme environmental conditions, due to the complex interplay of timing of tidal exposure and weather conditions (Admiraal 1984; Paterson and Hagerthey, 2001). Excessive light exposure generates intra-cellular oxidative stress (Roncarati *et al.*, 2008; Waring *et al.*, 2010) which can lower photosynthetic efficiency (i.e. photoinhibition; Wu *et al.*, 2012; Cartaxana *et al.*, 2013) and ultimately community-level primary productivity (Blanchard *et al*., 1996; Guarini *et al*., 2006). Furthermore, benthic diatom's photosynthesis often operates under the combined action of high light and other potentially stressful environmental factors such as extreme temperature (Blanchard *et al.*, 1997; Serôdio and Catarino, 1999). Although photosynthesis is known to be highly sensitive to temperature (Mathur *et al.*, 2014), effects of high temperature on MPB productivity, either alone or in combination with excess light have received little attention (Grant, 1986; Vieira *et al.*, 2013 and references therein). However, recent results showed implications on both dial and seasonal scales (Hancke *et al.*, 2014). On a longer term perspective, the cumulative effects of light and temperature could be relevant as well, as climate change is expected to influence not only average values but also the frequency and the intensity of extreme events such as heat waves (Schär *et al.*, 2004; Stott *et al.*, 2004; Solomon *et al*., 2007).

The actual photoinhibitory effects depend on the photoadaptive strategy of the diatoms of MPB, i.e. the operating efficiency of a range of mechanisms which include 'behavioural' and 'physiological' photoprotective processes (Barnett *et al.*, 2014). The 'behavioural photoprotection' consists of a strong negative phototaxis resulting in downward migration under supersaturating light intensities (Kromkamp *et al.*, 1998; Perkins *et al.*, 2010; Cartaxana *et al.*, 2011; Serôdio *et al.*, 2012). The vertical migration of cells within the steep light gradient of the sediment photic zone (Paterson and Hagerthey, 2001; Cartaxana *et al.*, 2011) has been hypothesized to allow for the optimization of light harvesting and the avoidance of excess light (Admiraal, 1984). Strong evidence for a photoprotective role of vertical migration was provided by the use of the diatom motility inhibitor Latrunculin A (Lat A) on undisturbed biofilms (Perkins *et al.*, 2010; Cartaxana *et al.*, 2011; Serôdio *et al.*, 2012). 'Physiological photoprotection' mainly includes the excess energy-dissipative non-photochemical quenching of chlorophyll (Chl) *a* fluorescence (NPQ). NPQ is mainly controlled by the presence of the xanthophyll pigment diatoxanthin (DT) and of Lhcx proteins in the light-harvesting complexes of photosystem II (PSII) (Depauw *et al.*, 2012; Lepetit *et al.*, 2012, 2013; Lavaud and Goss, 2014). In diatoms, DT is produced by the (dark/low light) reversible light-dependent conversion of the xanthophyll diadinoxanthin (DD) in the so called xanthophyll cycle (XC) (Goss and Jakob, 2010). Besides its involvement in NPQ, it seems to have another function as antioxidant (Lepetit *et al.*, 2010).

Despite the crucial role of NPQ and XC in the photoprotective response of diatoms to excessive fluctuating light regimes, especially in field situations (Brunet *et al.*, 2010; Lavaud and Lepetit, 2013; Lavaud and Goss, 2014), they have only scarcely been studied in MPB. They show a relation to diurnal and tidal cycles, season, latitude (Serôdio *et al.*, 2005; van Leeuwe *et al.*, 2008; Chevalier *et al.*, 2010), to vertical position of diatoms within the sediment (Jesus *et al.*, 2009; Cartaxana *et al.*, 2011) or along the intertidal elevation gradient

(Jesus *et al.*, 2009), with significant differences between the main growth forms (i.e. epipelic and epipsammic: Cartaxana *et al.*, 2011; Barnett *et al.*, 2014). As for the implication of Lhcx proteins in diatom NPQ, its characterization has been limited to few model species (Bailleul *et al.* 2010; Zhu *et al.*, 2010). Lhcx1 is involved probably at least by binding DT (Bailleul *et al.*, 2010; Büchel, 2014). It is present at low light and its transcript level/synthesis is slightly enhanced under high light (HL) (Bailleul *et al.*, 2010; Wu *et al.*, 2012; Lepetit *et al.*, 2013). While the transcript levels/synthesis of other examined isoforms (i.e. Lhcx2, Lhcx3, Lhcx6) strongly increase during HL (Zhu *et al.*, 2010; Lepetit *et al.*, 2013) and temperature stress (for Lhcx6; Wu *et al.*, 2012), their exact physiological role remains unknown, although Lhcx3 and Lhcx6 are suspected to be involved in the binding of *de novo* synthesized DT and/or the sustain part of NPQ (i.e. qI) during a prolonged HL stress (Zhu *et al.*, 2010; Lepetit *et al.*, 2013).

This work intended to study the combined effects of high light (HL) and high temperature on the photophysiology of intertidal diatom-dominated MPB communities. Light stress-recovery experiments (LSRE) were performed to distinguish physiological photoprotection efficiency from photoinhibitory effects, and to quantify behavioural photoprotection (Serôdio *et al.*, 2012). Until now, these processes have been characterized only to the extent of chlorophyll fluorescence measurements and XC pigments analysis. The present study combines chlorophyll fluorescence imaging, pigment analysis and for the first time on intact biofilms, lipid peroxidation quantification and immunodetection of Lhcx proteins. LSRE were performed on MPB from two locations in France and Portugal with different solar exposure and temperature regimes, likely to support the establishment of diatom communities with contrasting photo- and thermo-adaptive strategies. Moreover, the potential role of temperature in modulating the HL-induced stress was investigated by carrying out LSRE at two experimental temperature conditions (‘optimal’ *vs*. high temperature). In parallel, the

estimated photosynthetic and protective indices were further compared with field situation at the two sites during a typical summer diurnal emersion.

Results

Environmental conditions, in situ *photosynthetic activity and taxonomic composition of microphytobenthos in PT and FR sites*

Environmental conditions and MPB photosynthetic activity were assessed during typical summer diurnal emersion at both Portuguese (PT) and French (FR) intertidal flats. The Photosynthetic Active Radiation (PAR) reached its daily maximum (2000 µmol photons m^{-2} s^{-1}) at both sites (Fig. 1A-B) with a comparable light dose over the emersion (~19 to 23 mol photons m^{-2}, Table S1). Temperature was higher at PT site (Fig. 1A-B). Average temperatures at the sediment surface were 37.5°C and 28.8°C for PT and FR sites, respectively. Temperature decreased with sediment depth with a stronger effect in PT site (-7°C and -6°C in the first 0.5 cm for PT and FR sites, respectively: Table S1, Fig. 1A-B).

At the beginning of emersion, the effective PSII quantum yield (ΦPSII) was close to its optimum at both sites (~ 0.70: Fig. 1C-D, open squares). It decreased/increased opposite to the PAR evolution over the emersion period, reaching values as low as ~ 0.40. The maximal non-photochemical quenching of Chl *a* fluorescence (NPQ_{max}) was about 4-5 at PT site and lower than 1 at FR site at the beginning of emersion (Fig. 1C-D, closed circles). It decreased continuously at PT site to reach values around 3 at the end of the emersion, while it covaried with PAR at FR site, reaching a maximum value of about 6 (matching the sudden increase in PAR level) and values of 3-4 at the end of the emersion.

At both sites, MBP communities were dominated by epipelic (i.e. motile) benthic diatoms of the genus *Navicula* (Table S2). *Navicula phyllepta* sensu lato (Vanelslander *et al.*, 2009) was the dominant species at PT site (relative abundance: 44 %) while FR site was co-dominated by *N. spartinetensis* (33 %) and *N. phyllepta* s.l. (28 %).

Comparison between in situ *and experimental conditions*

The two temperature treatments used for the laboratory experiments during the LSREs were 27.4 ± 1.2°C and 37.3 ± 0.7°C (thereafter named 27°C and 37°C temperature treatments, respectively), which was close to the average temperatures monitored at the sediment surface for both sites (see above and Table S1). The light exposure of 3 h of 1200 µmol photons m^{-2} s^{-1} represented a light dose of 12.96 mol photons m^{-2} (Serôdio *et al.*, 2012). This light dose was reached after 2 h 53 min and 3 h 34 min in PT and FR sites, respectively (Table S1).

LSRE-induced photoinhibition and NPQ in sediment from FR site

ΦPSII remained constant in samples maintained under LL throughout the experiment (0.66 ± 0.02, Fig. 2). In comparison, samples exposed to HL exhibited dramatic changes over time (time: $P < 0.001$, see Table S3a for detailed statistical outputs). After 3h HL, ΦPSII decreased down to values between 0.13 ± 0.03 (37°C +Lat A) and 0.34 ± 0.02 (27°C Ctrl). It increased during LL recovery but did not reach back its initial level (0.46 ± 0.05 (37°C +Lat A) and 0.61 ± 0.01 (27°C Ctrl). The differences observed between temperature and chemical treatments were significant (temperature: $P < 0.001$; chemical: $P < 0.01$; Table S3a), and they both increased with time (time × temperature: $P < 0.001$; time × chemical: $P < 0.05$; Table S3a). Similarly, NPQ of samples maintained under LL remained constant (0.38 ± 0.04, Fig. 3) and changed over time according to light (time: $P < 0.001$, Table S3b): it increased under HL (between 4.4 ± 0.5 and 3.4 ± 0.4 from 37°C +Lat A and 27°C Ctrl treatments, respectively) but only partially relaxed during the subsequent 15 min LL incubation (between 1.9 ± 0.1 and 1.1 ± 0.1; Fig. 3). The effect of temperature was highly significant (temperature: $P < 0.001$, Table S3b) and the observed differences increased with time (time × temperature: $P < 0.001$; Table S3b). In comparison, the effect of lat A was less significant (chemical: $P < 0.05$ and time × temperature: $P = 0.11$; Table S3b).

LSRE-induced allomerization of Chl a *and xanthophyll cycle in sediment from FR site*

All samples exhibited typical diatom pigment signatures, including Chl *a*, Chls *c*, fucoxanthin, the carotenoid ß, ß carotene (data not shown) and the xanthophyll cycle pigments DD and DT. The allomer form of Chl *a* (Chl *a*-allo) accumulated during the LSRE as illustrated by the Chl *a* allomerization molar ratio (AR= Chl *a*-allo / total Chl *a* × 100, Fig. 4A). AR increased ~ 2-fold under HL and remained stable thereafter (time: $P < 0.001$; Table S3c). No significant changes were observed with temperature (temperature: $P = 0.48$; Table S3c), whereas AR was significantly higher in +Lat A samples than in Ctrl (chemical: $P < 0.01$; Table S3c), with mean maximum values of 11.9 ± 5.0% and 8.4 ± 2.1%, respectively (Fig. S1). AR did not significantly change in samples maintained in LL during 3 h (5.9 ± 2.7% on average).

The pool of DD+DT (in mol. 100 mol Chl a^{-1}) increased ~ 3-fold under HL and remained stable during the LL recovery (Fig. 4B, time: $P < 0.001$; Table S3d). Overall, it reached higher values at 37°C than at 27°C (temperature: $P < 0.01$; Table S3d) but it was comparable in Ctrl and +Lat A samples ($P = 0.58$; Table S3d). At 37°C, DD+DT increased even in the samples maintained under LL for 3 h (from 15.0 ± 4.0 to 23.8 ± 6.6 mol. 100 mol Chl a^{-1}, Tukey HSD: $P < 0.05$, Fig. S2). DD de-epoxidation (DES = DT / DD+DT × 100) correlated well with light whatever the temperature in both Ctrl and Lat A-treated samples ($P < 0.001$) (Fig. 4C-D). DES increased under HL and decreased during LL recovery while it remained stable in samples maintained in LL for 3 h (14.0 ± 3.2% on average) (Fig. S3). DES was significantly higher in +Lat A samples than in Ctrl ones (chemical: $P < 0.001$; Table S3d), and at 37°C than at 27°C (temperature: $P < 0.001$; Table S3d) with maxima of 67.2 ± 7.5% and 33.8 ± 7.5% at 37 °C and 27 °C, respectively, in +Lat A samples (Fig. S3). DES recovered much faster at 27°C than at 37°C, especially for Ctrl samples. In contrast to AR and the DD+DT pool, interaction between time and temperature was significant for DES (time ×

temperature: $P < 0.001$; Table S3d). Moreover, NPQ and DES were significantly positively correlated according to the chemical treatment (Ctrl/+Lat A), *i.e.* the slope of the NPQ *vs*. DES linear regression was 2.5 lower in +Lat A samples (Fig. S4) while for both treatments the origin of the regression was similar and non-nul (Ctrl: 17.6 ± 0.4; +Lat A: 16.4 ± 0.4), i.e. some DT was synthesized without NPQ development.

LSRE-induced Lhcx synthesis in sediment from FR site

The anti-FCP6 (i.e. Lhcx1) revealed a clear Lhcx isoform in FR samples (Fig. 5A). Its size of about 24 kDa was slightly higher than the one of Lhcx 3 in *Phaeodactylum tricornutum* and its amount increased after 3 h HL exposure especially in +Lat A samples. Interestingly, *N. phyllepta* s.l., the dominant species of the MPB assemblage, showed an Lhcx pattern similar to *P. tricornutum* so that three isoforms (Lhcx1, Lhcx2 and Lhcx3) could be identified. The anti-Lhcx6 from *Thalassiosira pseudonana* revealed two Lhcx isoforms in FR samples, the size of which was different from Lhcx6 and was neither present in HL exposed *P. tricornutum* cells (Fig. 5B). *N. phyllepta* showed two isoforms, one which size was slightly higher than Lhcx6 and the other one with a similar size to the 33-50 kDa isoform from FR samples. With such size, this isoform could be a hypothetic Lhcx dimer (given that the available sizes of Lhcx monomers deduced from the genomes of *P. tricornutum*, *T. pseudonana* and *Fragilariopsis cylindrus* range between 21 and 29 kDa) but different than in *P. tricornutum*. The 17-23 kDa isoform showed a size similar to Lhcx 1 in *P. tricornutum* and *N. phyllepta* (see Fig. 5A). Interestingly, the two isoforms reacted to light, temperature and Lat A in different ways: while the 17-23 kDa isoform appeared not to react to any of the treatments, the 33-50 kDa isoform positively reacted to HL and 37°C with an effect enhanced by Lat A at 37°C (Fig. 5C).

LSRE-induced lipid peroxidation in sediment from FR site

Common markers of membrane lipid peroxidation (TBARS-thiobarbituric acide reactive substances) were quantified. In Lat A treated samples, TBARS content normalized to the surface microphytobenthos biomass (I_{diat} biomass index) did not change significantly over time and was not significantly affected by chemical or temperature treatments (P = 0.71, 0.99 and 0.19, respectively; Table S3f), exhibiting a mean value of 1.19 ± 0.29 10^{-6} nmol eq MDA mL^{-1} (Fig. 6).

Comparison between FR and PT sites: NPQ, photoinhibition, lipid peroxidation and Lhcx.

ΦPSII and NPQ measured on PT samples at T0 (0.67 ± 0.02 and 0.40 ± 0.05, respectively) were comparable to the one measured on FR ones (Fig.2 and 3: 0.66 ± 0.01 and 0.39 ± 0.01, respectively), and they exhibited the same general trend under HL stress. However, PT samples were less affected by the HL treatment, as ΦPSII recovered faster under LL (site: $P < 0.001$, Table S4a), regardless of temperature or Lat A application (Fig. 7A). Moreover, NPQ did not relax entirely, but the level of this sustained NPQ was lower than in FR samples (site: $P < 0.01$, Table S4b), although post-hoc multiple comparison tests did not show any statistical differences between sites (Tukey HSD: $P > 0.05$; Fig. 7B).

For each site and temperature, the extent of photoinhibition and the contribution of vertical migration to the overall photoprotection capacity of MPB were estimated as in Serôdio *et al.* (2012) (Table 1). Photoinhibition was higher in FR than PT site but it increased similarly (~3 fold) with temperature. The contribution of vertical migration to photoprotection remained below 15 % but was always lower in PT biofilms (< 5%).

In Lat A treated samples, TBARS content normalized to surface biomass did not change significantly at PT site whatever the temperature (Fig. S5). Mean value was 3.26 ± 0.66 10^{-6} nmol eq MDA mL^{-1}, which was significantly higher than for FR samples (t-test: $P < 0.001$).

While the anti-FCP6 (i.e. Lhcx1) revealed two clear Lhcx isoforms in PT samples (Fig. 8), the anti-Lhcx6 did not bring any signal probably due to its unspecificity as regards to the species composing the microphytobenthic community of PT site. Their respective size were close with one at about 23 kDa, the size of Lhcx 3 in *P. tricornutum* and *N. phyllepta*, and the other one slightly higher (about 24 kDa) which was also present in FR samples (Fig. 5A). Both isoforms (although the 24 kDa reacted in a stronger way) were enhanced after 3 h of HL exposure as well as by the higher temperature; this effect was increased by the addition of Lat A. Interestingly, at 27°C, the 24 kDa isoform was not present under LL and HL exposure, it appeared with the addition of Lat A solely (LL 27°C +) and its content was increased by HL exposure (HL 27°C +). Similarly, the 23 kDa isoform positively reacted to Lat A to a level even similar to HL exposure without Lat A (compare 27°C LL+ and 27°C HL-).

Discussion

In this study, higher temperature significantly increased photoinhibition susceptibility of epipelic MPB biofilm. Communities from the Portuguese (PT) site were clearly more resistant to a coupled high light-temperature stress, in comparison to biofilms from the French (FR) site. At both site, photoprotection was based on the interplay between physiological (NPQ, DT and Lhcx proteins) and behavioural (vertical motility) response, nevertheless PT biofilms displayed a lower relative contribution of vertical migration and a stronger NPQ. The apparent latitudinal pattern observed at the community level ('MPB biofilm') might be driven by the individual response of the respective dominant diatom species/ecotypes in each site. These different aspects are discussed below.

Evidence for a latitudinal adaptation in the response of epipelic MPB to a coupled light-temperature stress

Our results suggest that PT MPB communities were adapted to a higher light and/or temperature environment than FR ones. Overall, PT samples were more resistant than FR ones to HL stress, regardless the effect of temperature. At 27°C, PT control samples recovered almost entirely from HL exposure (97 %), and photoinhibition increased only from 3 to 10 % at 37°C. This trend was also obvious *in situ*: the time course and level of ΦPSII were comparable between sites despite the potentially more stressful conditions at PT site (similar light conditions but 8-9°C higher average surface temperature). One of the reasons for this differential latitudinal adaptation might lie in the photoprotective strategies the two MPB communities exhibited. PT MPB communities showed higher NPQ_{max} average values, an indication of a strong(er) physiological photoprotective response (Serôdio *et al.*, 2005). PT NPQ_{max} was already high right from the beginning of the emersion although light intensity was still moderate and it remained relatively stable along the emersion. Consequently, vertical

migration contributed less to the overall photoprotection capacity (< 5 %) in comparison to FR biofilms. FR NPQ_{max} tended to follow the fluctuations of light intensity along the emersion which would be in agreement with a more dynamics MPB response, regarding both motility and physiology. Only few studies have examined the link between seasonal and/or latitudinal photoacclimation and the coupling between behavioural and physiological photoprotection in MPB communities. A similar increase of migration contribution was reported for communities acclimated to lower irradiances (i.e. seasonal acclimation: Serôdio *et al.*, 2012). Another study provided evidence for the differential role of migration *vs*. XC along a latitudinal gradient (Ireland, UK and Portugal), although the role of sediment type (i.e. mud *vs*. sand) could not be ruled out (van Leeuwe *et al.*, 2008).

In contrast, the contribution of thermal adaptation is difficult to ascertain. Although PT samples were more resistant and resilient, higher temperature leads to comparable effects: photoinhibition increased to about 3-times (i.e. from 3 to 10 % and from 8 to 22 %, in PT and FR sites, respectively) and lipid peroxidation was comparable. The pattern of the detected Lhcx isoforms was also similar, although no quantification was possible. Average surface and -0.5 cm temperature conditions experienced by the FR and PT communities were clearly different. The fact that this difference was lower than the observed amplitude over an emersion could explain the apparent lack of temperature latitudinal pattern. This is in agreement with other comparative studies on short-term (i.e. over few hours) temperature effects on MPB photosynthesis (Grant, 1986; Blanchard *et al.*, 1997; Hancke and Glud, 2004). Instead, the different average temperature conditions at PT and FR sites recorded in this study, which are representative of typical summer conditions in these areas (Guarini *et al.*, 1997; Lillebo *et al.*, 2010), might have played a role on a longer time scale. As temperature and light adaptations rely on similar strategies (Davison, 1991; this study, see below), it is likely that the difference in average temperatures influenced the susceptibility of

MPB to photoinhibition, directly and/or via its photoacclimation status, together with e.g. daily light dose, day length and/or UV exposure.

The latitudinal pattern in ecophysiological characteristics observed at the community level coincided with a shift in the diatom species composition. Although it is difficult to separate 'community' response from 'individual species' response within the biofilm, it is possible that the observed responses at each site were driven by the few dominant species (representing c.a. 50% of the total abundance). The two dominant species, *N. phyllepta* s.l. and N. *spartinetensis*, are known to be widespread along the European Atlantic and Northwestern coasts (Vanelslander *et al*., 2009; Witkowski *et al*., 2012). Epipelic diatoms generally exhibit a low NPQ, in comparison to non-motile ones (Barnett *et al.*, 2014). This does not preclude the existence of interspecific variability between organisms sharing the same life style, considering both behavioural (Underwood *et al.*, 2005; Du *et al.*, 2010, 2012) and physiological photoprotective mechanisms (Barnett *et al.*, 2014). Furthermore, the occurrence of *N. phyllepta* s.l. at both sites can be explained by the pseudocryptic feature of this taxonomic group. It comprises different closely related species morphologically indistinguishable but exhibiting important ecophysiological differences and environmental preferences (Vanelslander *et al*., 2009). To which extent the differences observed between PT and FR sites (i.e. stronger NPQ_{max} in PT assemblage regardless of the stress treatment; different Lhcx patterns) can be explained by the differential relative abundances of *N. phyllepta* s.l. vs. *N. spartinetensis* and/or pseudopcryptic species or ecotypes of *N. phyllepta* s.l is a question that remains to be answered.

Higher temperature increases photoinhibition susceptibility in epipelic MPB

To our knowledge, this is the first study which shows that on intact migratory MPB biofilms high temperature and HL acts synergistically in decreasing photosynthesis, a feature so far

reported only for individual species (Salleh and McMinn, 2011). Other works have shown that temperature alone impacts photosynthesis in benthic diatoms, in monospecific cultures (Morris and Kromkamp, 2003; Yun *et al.*, 2010), MPB suspensions (Blanchard *et al.*, 1997), and intact MPB biofilms (Vieira *et al.*, 2013). In conditions where photosynthesis is light-saturated, benthic diatom photosynthesis can respond to a transient temperature increase if it remains within a 25-35°C range. The high temperature used here (37.3 ± 0.7°C) falls slightly outside this range, a situation likely to occur regularly *in situ* in summer, as confirmed by our field data.

In situ measurements showed that ΦPSII correlated well with irradiance during the emersion period. During LSRE, a strong decrease was also observed after 3 h of HL exposure. Although the applied light dose was lower than *in situ*, our results show that it was strong enough to induce photoinhibition at the community level. The incomplete recovery of ΦPSII after 15 min LL coincided with a sustained phase of NPQ which was induced during the prolonged HL exposure. This can be partly attributed to photoinhibition and illustrates the physiological response to harsh stress (Zhu *et al.*, 2010; Wu *et al.*, 2012; Lavaud and Lepetit, 2013). At optimal temperature (27°C; see Blanchard *et al.*, 1997 and Experimental procedures section), photoinhibition remained below 20 %, which is consistent with a previous study using a similar experimental approach (Serôdio *et al.*, 2012). Photoinhibitory effects may be attributed to the progressive accumulation of reactive oxygen species (ROS, Roncarati *et al.*, 2008; Waring *et al.*, 2010), as evidenced by the increase of AR at the end of LSRE. Indeed, ROS have been shown to be directly involved in Chl *a* allomerization (Hynninen *et al.*, 2010 and references therein). This is also consistent with the accumulation of Chl *a* allomers in response to oxidative stress in the diatom *P. tricornutum* (Cid *et al.*, 1995). When superimposed to HL stress, significantly increased photoinhibition (c.a. 3-times increase in the controls from 27 to 37°C) which is not surprising as PSII is the most thermosensitive

component of the photosynthetic apparatus (Mathur *et al.*, 2014). Nevertheless, the amount of MDA and other aldehydes (TBARS) were not affected, suggesting that antioxidant activities were sufficient to prevent from substantial ROS-mediated membrane damage during the 3 h stress exposure, even when migration was inhibited. In such short-term experiments (i.e. < 24 h), it seems that only stronger oxidative stress such as UV- or herbicides-induced leads to noticeable lipoperoxidation (Rijstenbil, 2005; Wang *et al.*, 2011).

New evidences on the interplay between behavioural and physiological response to light-temperature stress in epipelic microphytobenthos

In response to HL alone, diatoms which were free to move (i.e. in the controls) could reach deeper layers of sediment with lower light conditions, potentially closer to their photosynthetic optimum (Kromkamp *et al.*, 1998). This downward migration contributed to a reduction of the deleterious effects of HL observed in Lat A treated samples (i.e. immobilized cells at the surface of sediment) such as an enhanced accumulation of Chl *a* allomers and a slower ΦPSII recovery. Our results are in agreement with previous works using Lat A on natural biofilms (Perkins *et al.*, 2010; Serôdio *et al.*, 2012). Similarly, the motile diatoms could reach a depth with lower and more stable temperature, as shown by the *in situ* temperature depth profiles monitored here. Nevertheless, our measurements were not refined enough to conclude about the steepness of the vertical temperature gradient in muddy sediment, as for light (Paterson and Hagerthey, 2001; Cartaxana *et al.*, 2011). Additionally, high temperature alone is known to directly affect the motility of MPB diatoms, i.e. over 35°C cell motility significantly drops-down (Cohn *et al.*, 2003; Du *et al.*, 2012). Such feature might partly explain the stronger photoinhibition observed at 37°C in Lat A free samples, together with a direct impact of temperature on physiological mechanisms.

NPQ developed in the same range of mean values (i.e. 3-4) *in situ* than during LSRE with HL stress alone. Concomitantly, the DD+DT pool size as well as DES increased. DT synthesis was based not only on DD de-epoxidation (as illustrated by DES) but also by additional DT *de novo* synthesis (Lavaud and Lepetit, 2013; Lepetit et al., 2013) which enlightened the high level of stress the cells were exposed to. Whatever the source, additional DT provides higher physiological photoprotection via higher NPQ and/or via higher prevention of oxidative lipid peroxidation (Lepetit et al., 2010; Lavaud and Lepetit, 2013). DT synthesis (DD+DT and DES) is enhanced by the high temperature stress alone (Salleh and McMinn, 2011), and this effect was even stronger in conditions of a coupled HL and high temperature stress. Specifically, DD+DT and DES showed a slower recovery which could represent a feed-back reaction (i.e. related to HL/high temperature impairment of the Calvin cycle activity, Mathur *et al.*, 2014) for the maintenance of a photoprotection capacity to cope with prolonged stressful temperature conditions, even under LL (Lavaud and Lepetit, 2013; Lepetit *et al.*, 2013). When the diatom motility was inhibited by Lat A, DES significantly increased independently of the temperature, and its recovery was slower. This was apparently not due to a higher DT *de novo* synthesis as illustrated by the similar DD+DT pool size with and without Lat A. Higher DT synthesis in presence of Lat A had no significant effect on NPQ, except for its increased sustainability when in conjunction with high temperature. Higher sustained NPQ (i.e. qI) is known to be related with both sustained DT and photoinhibition in conditions of a strong stress (Lavaud and Lepetit, 2013; Lepetit et al., 2013). As a consequence, the DT quenching efficiency (i.e. the slope of the NPQ-DT relationship) was lower in presence of Lat A, likely due to the differential involvement of DT molecules in NPQ (Lavaud and Lepetit, 2013): in presence of Lat A, the additional DT molecules instead most probably acted as ROS scavengers in prevention of lipid peroxidation (Lepetit *et al.*, 2010) arguing for a pronounced stress (i.e. HL + hight temperature + inhibition of motility) level.

Although, as expected, the Lhcx pattern in sediment samples was not as clear as the one of monocultures of *N. phyllepta*, one of the dominant species common to the FR and PT MPB communities, the confirmation of the presence of some of the known isoforms was possible. While an isoform with a similar size than Lhcx1 apparently did not react to any of the treatments, we found that the synthesis of two isoforms were enhanced by HL, high temperature and Lat A: one isoform with a size similar to Lhcx3, and one isoform with the size of a dimer which especially positively reacted to high temperature and Lat A treatment. Interestingly, these two isoforms were also present in *N. phyllepta*. A third isoform (of about 24 kDa), which was not detected in *N. phyllepta*, was synthetized in all treatments. Based on our knowledge of the synthesis and roles of Lhcx proteins during prolonged stress, it is reasonable to argue that these isoforms participated, at least in part, to the above described NPQ and XC patterns during the coupled HL and high temperature stress. Interestingly, the Lhcx3 and 24 kDa isoforms strongly reacted to Lat A out of any stress and to a level comparable to HL stress. It suggests that the inhibition of motility might generate a strong preventive physiological answer in diatom cells blocked at the surface of sediment (which can occur *in situ* during sediment desiccation events for instance), an additional hint that physiological and behavioural photoprotection are closely related in epipelic diatoms. This compensation, together with a stronger NPQ induction and XC activity, was nevertheless not strong enough to prevent immobilized cells from additional photoinhibition, as ΦPSII recovery was always lower in Lat A treated samples than in migratory biofilms.

Conclusions and perspectives

By using a number of methodological novelties in MPB research (a new cryo-sampling method, lipid peroxidation markers for photooxidative stress-TBARS, photosynthetic protein

markers for physiological protection-Lhcx), the present study clearly strengthens the previous statement of a coupled and complementary action of physiological and behavioural processes in protecting the photosynthetic activity of MPB diatoms in stressful environmental conditions (Perkins et al., 2010, Cartaxana et al., 2011; Serôdio et al., 2012). Moreover, our results bring a physiological basis to the previously reported depression of MPB photosynthetic productivity in summer (Guarini et al., 1997). They emphasize the joint role of temperature and light in limiting, at least transiently (i.e. during emersion), the photosynthetic activity of MPB biofilm *in situ*. They confirm that high temperature, together with high light, is an important environmental driver which supports seasonal, spatial and potentially latitudinal MPB biodiversity and biomass distribution at the scale of intertidal mudflats along the Atlantic coast of Southern Europe (Guarini et al., 1997; Brito et al., 2013).

Moreover, temperature being expected to increase due to global change (Solomon *et al.*, 2007), further longer-term experiments are required in order to question its importance in modulating MPB photosynthetic activity. Our results support previous works suggesting that MPB gross photosynthesis will most probably not be affected by a small increase (even if significant, i.e. +1°C to +4°C for the most extreme previsions; Solomon *et al*., 2007) of average temperature (Vieira *et al.*, 2013; Hancke *et al.*, 2014). However, it does not preclude a potential change in the community structure, as observed for associated invertebrate assemblages (Hicks *et al.*, 2011), which might be of importance in driving the whole community response as reported here. Further experiments should rather focus on the cumulative effects of successive extreme events such as heat waves experienced during spring/summer (Schär *et al*., 2004; Stott *et al*., 2004), with an emphasis on the 'species/individual' *vs*. 'community/biofilm' response.

Experimental procedures

Study areas and experimental design

Two intertidal mudflats were sampled along the Atlantic Coast of Southern Europe, in France and Portugal (FR and PT sites, respectively): a macrotidal one in the Baie de l'Aiguillon near Esnandes (FR, 46°15.36'N, 1°8,55'W) and a mesotidal estuary in the Ria de Aveiro near Vista Alegre (PT, 40°35' N, 8°41' W). Both sites are composed of fine muddy sediments (dominant particle size < 63 µm) and are known to be colonized by epipelic diatom-dominated MPB throughout the year (Haubois *et al*., 2005; Serôdio *et al.*, 2012, respectively).

All experiments were performed consecutively in early summer (weeks 26-27, June-July 2012). For each site, natural migratory MPB was studied *in situ* over one diurnal emersion period. In parallel, light stress-recovery experiments (LSRE) were carried out in controlled conditions in the laboratory at two temperatures using freshly collected samples (see section below). During LSRE, samples were sequentially exposed to (i) low light (LL) level to determine pre-stress reference state; (ii) high light (HL) intensity to induce photoinhibitory effects; (iii) LL to monitor recovery from HL stress (Serôdio *et al.*, 2012).

In situ *measurements*

For each site, the day for carrying out the experiment was selected so that the emersion period matched with maximum light and temperature exposure, i.e. noon/early afternoon low tides. Photosynthetic Active Radiation (PAR) and temperature at the surface of the sediment were assessed every 30 s with a universal light-meter and data logger (ULM-500, Walz Effeltrich Germany) equipped with a plane light/temperature sensor (accessory of the ULM-500) and a plane cosine quantum sensor (Li-COR). Depth temperature profiles were measured with Hobo sensors (Hobo Pro V2, Massachussets, USA) fixed on a home-made stick that was vertically inserted into the sediment to position the sensors at four (-0.5 cm, -2 cm, -5 cm, -10 cm). The

effective photosystem II quantum yield (ΦPSII) and the non-photochemical quenching of chlorophyll *a* (Chl *a*) fluorescence (NPQ) of MPB was assessed with a Water-PAM (micro-fiber version, Walz GmbH, Effeltrich, Germany) as described in Lefebvre *et al.* (2011). ΦPSII was calculated as $\Delta F / F_m' = (F_m - F) / F_m'$. Rapid light curves (RLCs) with 30 s light steps were used to measure NPQ *vs* irradiance (NPQ-E) curves (as recommended in Lefebvre *et al.*, 2011). NPQ-E curves were fitted with the model by Serôdio and Lavaud (2011) in order to estimate NPQ_{max} where $NPQ = (F_m - F_m') / F_m$. F_m and F_m' are the maximum Chl *a* fluorescence levels measured in dark-adapted and illuminated (at the end of each RLCs light steps) MPB, respectively, while F is the steady-state Chl *a* fluorescence level measured at the end of each RLC light step, just before F_m' was assessed. F was measured with the application of a non-actinic modulated beam of 455 nm, and F_m and F_m' with the application of over-saturating (about 4000 µmol photons m^{-2} s^{-1}) light pulses (800 ms). Because in *in situ* as well as in laboratory (see below) conditions (i.e. light-responsive migratory biofilm) it is virtually impossible to measure a true F_m level, for the calculation of NPQ, F_m was in reality the maximum F_m' of the respective RLC (i.e. $F_m'_{max} \sim F_m$, see Lefebvre *et al.*, 2011).

Light stress-recovery experiments (LSRE)

LSRE were carried out following a protocol adapted from Serôdio *et al.* (2012). The top 1 cm of sediment was collected at the beginning of low tide and immediately transported to the laboratory where it was sieved (0.5 mm mesh) to remove debris and macrofauna. Sediment was thoroughly mixed and spread in trays, forming a 2-4 cm thick slurry, and it was covered with seawater from the sampling site and left undisturbed overnight in the dark at room temperature (~20-25°C). The next morning, the slurry was homogenized and transferred to 24-well plates using a 100 mL syringe, filling the wells completely (ca. 3 mL). The well plates were then exposed to constant LL of 50 µmol photons m^{-2} s^{-1}, provided by three slide

projectors (Reflecta Diamator AF, Reflecta GmbH, Rottenburg, Germany) containing halogen lamps (Quartzline DDL 150W, General Electric, USA) to induce the upward migration of MPB. Once the MPB biofilm was formed (typically after 3 h), the plates were transferred to a water bath of constant temperature of 25°C or 40°C and exposed to constant LL for 30 min. These two experimental temperatures were defined based on a previous study (Blanchard *et al.*, 1997) which defined 25°C as an optimum and 35-40°C as an extreme maximum for the photosynthetic productivity of MPB. A fixed volume (200 µL) of Lat A solution (10 µM final concentration) or of filtered sea water (Control samples: Ctrl) was added to each well. Lat A solution was freshly prepared daily from a 1 mM stock solution of purified Lat A (Sigma-Aldrich) dissolved in dimethylsulfoxide and stored at -20°C (Cartaxana and Serôdio, 2008). After 15 min waiting for the inhibitor to diffuse, the plates were exposed to HL (1200 µmol photons m^{-2} s^{-1}, 3 h). This light dose (12.96 mol photons m^{-2}) was previously shown to be excessive for MPB photosynthesis (Serôdio *et al.*, 2012). After 3 h, samples were placed under LL for 15 min. In parallel, additional samples (for both Ctrl and +Lat A treatments) were maintained during 3 h under continuous LL. Temperature of the sediment in the top 5 mm was regularly checked using the same sensor previously described. The duration of each step described above was always the same, but the timing was adjusted so that HL period always started at the low tide maximum expected *in situ*.

For each chemical and light treatment (Ctrl and +Lat A; HL or continuous LL), several endpoints were assessed on 3-6 independent samples at three times: just before the HL stress (T_0), at the end of the HL stress and after 15 min of LL recovery (Recov). For the experiments with FR samples, Chl *a* fluorescence was measured using an Imaging-PAM fluorometer (Maxi-PAM M-series, Walz GmbH, Effeltrich, Germany) and samples were collected for further quantification of photosynthetic pigments, lipid peroxidation, and Lhcx proteins. For PT samples, Chl *a* fluorescence was measured with a FluorCAM 800MF, open version (PSI,

Brno, Czech Republic, see Serôdio *et al.*, 2013). Samples were collected for the same analyses than for FR site, except that pigments were not quantified. Samples were collected for the same analyses than for FR site, except that pigments were not quantified. ΦPSII and NPQ were calculated as previously described (Serôdio *et al.*, 2012).

For the sediment sampling in wells, a contact-corer specially designed was used to collect rapidly (< 30 s) the uppermost layer of sediment (0.5 mm thick, 1.5 cm^2 area) in each well. It is based on the cryo-sampling of the biofilm, through the contact of the sediment surface with a metal cylinder of known length previously cooled in liquid nitrogen (Laviale *et al.*, submitted). Each core was immediately frozen in liquid nitrogen and stored at -80°C until further analysis.

Pigment analysis

Pigment extraction and HPLC analysis were carried out following Lepetit *et al.* (2013), with the exception of the first extraction step which was performed after 24 h lyophilisation of the sediment cores (3 mL of 4°C mixture extraction buffer: 90% methanol/0.2 M ammonium acetate (90/10 vol/vol) + 10% ethyl acetate). Extracted samples were analyzed with a Hitachi LaChrom Elite HPLC system equipped with a 10°C-cooled autosampler and a Nucleosil 120-5 C18 column (Macherey-Nagel). The allomerization of Chl *a* was calculated as the ratio AR = Chl *a*-allo / tot Chl *a* × 100 where tot Chl *a* = (Chl *a*-allo + Chl *a*' + Chl *a*) and Chl *a*-allo and Chl *a*' are the allomer and epimer forms of Chl *a*, respectively. The pigment molar concentrations (expressed as mol. 100 mol Chl a^{-1}) for the xanthophyll cycle (XC) pigments diadinoxanthin (DD) and diatoxanthin (DT) were used to calculate the DD de-epoxidation state (DES) as follows: DES = [DT / (DD + DT)] × 100.

Lipid peroxidation

Lipid peroxidation generated by oxidative stress was estimated by quantifying thiobarbituric acide reactive substances (TBARS) according to Kwon and Watts (1964). Each sample was resuspended in 0.8 mL of 10% trichloroacetic acid (TCA, Sigma-Aldrich) and 500 mg L^{-1} butylated hydroxytoluene (BHT, Sigma-Aldrich) and sonicated (U200S control; IKA Labortechnik, Ika-Werke GmbH, Staufen, Germany) on ice 5 times during 30 s (cycle: 1, amplitude: 30%) with intervals of 30 s to prevent overheating. After extraction, 0.8 mL of 0.5% thiobarbituric acid (TBA, Sigma-Aldrich) in 10% TCA was added. The mixture was heated for 30 min at 90 °C and immediately put on ice to stop the reaction. Samples were then centrifuged (15 min, 10000 g) and 250 µL of supernatant were transferred in a 96 well-plate (Sarsted). TBARS were measured by subtracting the nonspecific turbidity (at 600 nm) from the TBARS absorption maximum (532 nm) using a Synergy HT absorbance microplate reader (BioTek Instruments Inc., Vermont, USA). Blanks consisted of the same mixture without sediment sample. TBARS concentration was expressed in malondialdehyde (MDA) equivalent (nmol mL^{-1}) using an extinction coefficient of 155 mM^{-1} cm^{-1}. As it was not possible to obtain paired measurements of Chl *a* and MDA, values were normalized to the microphytobenthos biomass present at the sediment surface (measured by spectral reflectance: see below). As migration was susceptible to occur in Ctrl samples, only Lat A-treated samples could be compared.

MPB surface biomass

MPB biomass present in the surface layers of the sediment was estimated by spectral reflectance analysis with a fiber optic spectrometer (USB2000-VIS-NIR, grating #3, Ocean Optics, Duiven, The Netherlands) according to Serôdio *et al.* (2009). In particular, measurements were carried out under LL (50 µmol photons m^{-2} s^{-1}) supplied with an halogen lamp (120W, Plusline ES, Philips Lighting) positioned with a 45° angle to the sediment

surface while the sensor was at a fixed distance (~2 cm) perpendicularly to it. Reflectance measurements at 550, 600 and 675 nm (ρ_{550}, ρ_{600} and ρ_{675}, respectively) were used to calculate the normalized index I_{diat} as follows: $I_{diat} = 2 \times \rho_{600} / (\rho_{550} + \rho_{675})$ (modified from Kazemipour et al 2012). It is based on the spectral peak centered at 600 nm between the absorbance bands due to the fucoxanthin at 550 nm and the Chl *a* at 675 nm. In comparison to other MPB spectral indices available (Méléder *et al.*, 2010), it was shown to be less affected by water or detritical organic matter contents, thus allowing a better comparison between sites (data not shown).

Lhcx protein analysis

Protein extraction from sediment cores, SDS-PAGE, Western-blot and ECL immunodetection were carried out following the protocol by Coesel et al. (2009) modified by Lepetit *et al.* (2013): In order to improve the proteins extraction, sediment samples were exposed to eight freeze thaw cycles in the extraction buffer (500 µL lysis buffer + 500 µL protease inhibitor, Sigma-Aldrich, USA) and then incubated at RT (total extraction was 90 min). Chl *a* concentration of extracted samples was determined according to Jeffrey and Humphrey (1975) and samples corresponding to an amount of 0.5 µg Chl *a* were loaded on the gel. Correct blotting was verified by correct transfer of pre-stained protein markers on the PVDF membrane (Amersham Hybond-P, GE Healthcare life Sciences, USA) and by staining gels with Coomassie R-250 (Pierce Imperial Protein stain, Thermo scientific, Rockford, USA). Anti-FCP6 (Lhcx1) from *Cyclotella cryptica* (Westermann and Rhiel, 2005) and anti-Lhcx6 from *T. pseudonana* (Zhu and Green, 2010) were applied in a 1:1000 dilution for LR samples overnight (respective incubations with the secondary antibody were 2 h and 1 h). For PT samples, the anti-Lhcx6 antibody did not yield a good signal; anti-FCP6 was used at a dilution of 1:1000 (incubation with the secondary antibody, 1 h). Note that because of the species-

specific immunodetection pattern no quantification *per se* was possible. However, the comparison with the planktonic models *P. tricornutum* (Bailleul *et al.*, 2010; Lepetit *et al.*, 2013) and *T. pseudonana* (Zhu *et al.*, 2010) enabled to possibly distinguish different isoforms including some for which behaviour under HL and temperature stress and their role is known or suspected (see Introduction; Bailleul *et al.*, 2010; Zhu *et al.*, 2010; Lepetit *et al.*, 2013; Büchel, 2014). For *P. tricornutum*, *T. pseudonana* and *N. phyllepta* samples, the procedure was as in Lepetit *et al.* (2013): exponentially growing cells were exposed to HL stress (2 h at 2000 µmol photons. m^{-2}. s^{-1}) to induce protein expression of several Lhcx isoforms which were separated on the LDS-gel.

Taxonomic composition

For each site, the first cm of sediment was collected and stored at -20 °C until analysis. Extraction from sediment of the organic fraction, including microalgae cells, was done following Méléder *et al.* (2007). Preliminary observations of the organic fraction using optical microscopy (Olympus AX70 using 200-fold magnification) were performed to confirm the absence of other classes of microalgae than diatoms. Permanent slides of cleaned diatom frustules (cremation: 2 h at 450 °C) were then prepared in a high refractive index medium (Naphrax; Northern Biological Supplies Ltd, Ipswich, UK). The taxonomic composition was determined to the species level by examining 200-300 frustule valves at 500 fold magnification on the basis of morphological criteria using reference works (Ribeiro *et al.*, 2013, and references therein). Scanning electron microscopy was used to confirm the analysis (JEOL JSM 7600F reaching 50 000-fold magnification).

Statistics

Data presented are mean ± one standard deviation (SD). Each LSRE experiment was performed twice. Analyses of variance (ANOVA), Tukey's honestly significant difference (HSD) tests, Student's t-tests and linear regressions were performed using the R statistical computing environment (v 2.15.1, Ihaka and Gentleman, 1996). In particular, potential interactions between factors were tested considering data set from each site individually, with time (T_0, after 3 h of HL, after 15 min recovery under LL), temperature (27°C and 37°C) and chemical (Ctrl or +Lat A) as fixed factors. The fact that Chl *a* fluorescence measurements were made on the same samples over the experiment was also taken into account using the sample name as random effect in a linear mixed effect model (lme function of the nlme package: Pinheiro and Bates, 2000). Comparisons between sites (FR, PT) were performed on data gathered at the end of the LSRE (after recovery), expressed as % of T_0. Site, temperature and chemical were considered as fixed factors. Data normality (Shapiro-Wilk test) and homoscedasticity (Bartlett test) were checked using the residuals.

Acknowledgements

The present study was supported by the Egide/Campus France-PHC Pessoa exchange program (n°27377TB, JL and JS), the Centre National de la Recherche Scientifique-CNRS (JL), the University of La Rochelle-ULR and the Contrat Plan Etat Région-CPER 'Littoral' (JL, BL post-doc grant), the Region Poitou-Charentes (AB Ph.D. grant), the Deutscher Akademischer Austausch Dienst-DAAD (BL post-doc grant), European Funds through COMPETE, the Portuguese Science Foundation (FCT) through projects PEST (PEst-C/MAR/LA0017/2013) and MigROS (PTDC/MAR/112473/2009: JS, ML post-doc grant and SF research assistant grant), and through grants SFRH/BSAB/962/2009 (JS), SFRH/BD/44860/2008 (JE Ph.D. grant). The authors thank Dr. E. Rhiel (Univ. Oldenburg, Germany) and Prof. B. Green (Univ. British Columbia, Canada) for the kind gifts of the anti-FCP6 and of the anti-Lhcx6, respectively, Prof. B. Green for her help analyzing the Lhcx6 Western-blot, C. Pais for her technical assistance with the TBARS quantification, Dr L. Ribeiro (Univ. Lisboa, Portugal) for his help in confirming the identification of *N. phyllepta* s.l., and Sr Armindo do Evaristo for his cheerful support. We thank the two anonymous reviewers for their constructive comments on the manuscript.

References

Admiraal, W. (1984) The ecology of estuarine sediment inhabiting diatoms. *Prog Phycol Res* **3**: 269-322.

Bailleul, B., Rogato, A., de Martino, A., Coesel, S., Cardol, P., Bowler, C. et al. (2010) An atypical member of the light-harvesting complex stress-related protein family modulates diatom responses to light. *Proc Natl Acad Sci USA* **107**: 18214-18219.

Barnett, A., Méléder, M., Blommaert, L., Lepetit, B., Gaudin, P., Vyverman, W. et al. (2014) Growth form defines physiological photoprotective capacity in intertidal benthic diatoms. *ISME J* doi:10.1038/ismej.2014.105.

Blanchard, G.F., Guarini, J.M., Gros, P., and Richard, P. (1997) Seasonal effect on the relationship between the photosynthetic capacity of intertidal microphytobenthos and temperature. *J Phycol* **33**: 723-728.

Blanchard, G.F., Guarini, J.M., Richard, P., Gros, P., and Mornet, F. (1996) Quantifying the short-term temperature effect on light-saturated photosynthesis of intertidal microphytobenthos. *Mar Ecol Prog Ser* **134**: 309-313.

Brito, A.C., Benyoucef, I., Jesus, B., Brotas, V., Gernez, P., Mendes, C.R. et al. (2013) Seasonality of microphytobenthos revealed by remote-sensing in a South European estuary. *Cont Shelf Res* **66**: 83-91.

Brunet, C., and Lavaud, J. (2010) Can the xanthophyll cycle help extract the essence of the microalgal functional response to a variable light environment? J *Plankton Res* **32**: 1609-1617.

Büchel, C. (2014) Fucoxanthin-chlorophyll-proteins and non-photochemical fluorescence quenching in diatoms. In *Non-Photochemical Fluorescence Quenching and Energy Dissipation In Plants, Algae and Cyanobacteria*. Demmig-Adams, B., Garab, G., Adams, W.W.III, and Govindjee (eds). Advances in Photosynthesis and Respiration, Volume 40.,

pp 259-275. Dordretch, The Netherlands: Springer.

Cartaxana, P., and Serôdio, J. (2008) Inhibiting diatom motility: a new tool for the study of the photophysiology of intertidal microphytobenthic biofilms. *Limnol Oceanogr-Meth*. **6**: 466-476.

Cartaxana, P., Ruivo, M., Hubas, C., Davidson, I., Serôdio, J., and Jesus, B. (2011) Physiological versus behavioral photoprotection in intertidal epipelic and epipsammic benthic diatom communities. *J Exp Mar Biol Ecol* **405**: 120-127.

Cartaxana, P., Domingues, N., Cruz, S., Jesus, B., Laviale, M., Serôdio, J., and da Silva, J.M. (2013) Photoinhibition in benthic diatom assemblages under light stress. *Aquat Microb Ecol* **70**: 87-92.

Chevalier, E.M., Gévaert, F., and Créach, A. (2010) In situ photosynthetic activity and xanthophylls cycle development of undisturbed microphytobenthos in an intertidal mudflat. *J Exp Mar Biol Ecol* **385**: 44-49.

Cid, A., Herrero, C., Torres, E., and Abalde, J. (1995) Copper toxicity on the marine microalga *Phaeodactylum tricornutum* - Effects on photosynthesis and related parameters. *Aquat Toxicol* **31**: 165-174.

Coelho, H., Vieira, S., and Serôdio, J. (2011) Endogenous versus environmental control of vertical migration by intertidal benthic microalgae. *Eur J Phycol* **46**: 271-281.

Coesel, S., Mangogna, M., Ishikawa, T., Heijde, M., Rogato, A., Finazzi, G., Todo, T., Bowler, C., Falciatore, A. (2009) Diatom PtCPF1 is a new cryptochrome/photolyase family member with DNA repair and transcription regulation activity. *EMBO Rep* **10**: 655–661.

Cohn, S.A., Farrell, J.F., Munro, J.D., Ragland, R.L., Weitzell, R.E., and Wibisono, B.L. (2003) The effect of temperature and mixed species composition on diatom motility and adhesion. *Diatom Res* **18**: 225-243.

Consalvey, M., Paterson, D.M., and Underwood, G.J.C. (2004) The ups and downs of life in a benthic biofilm: Migration of benthic diatoms. *Diatom Res* **19**: 181-202.

Davison, I.R. (1991) Environmental effects on algal photosynthesis - Temperature. *J Phycol* **27**: 2-8.

Depauw, F.A., Rogato, A., d'Alcala, M.R., and Falciatore, A. (2012) Exploring the molecular basis of responses to light in marine diatoms. *J Exp Bot* **63**: 1575-1591.

Du, G.Y., J.H., O., Li, H., and Chung, I.K. (2010) Effect of light and sediment grain size on the vertical migration of benthic diatoms. *Algae* **25**: 133-140.

Du, G.Y., Li, W.T., Li, H.B., and Chung, I.K. (2012) Migratory responses of benthic diatoms to light and temperature monitored by chlorophyll fluorescence. *J Plant Biol* **55**: 159-164.

Goss, R., and Jakob, T. (2010) Regulation and function of xanthophyll cycle-dependent photoprotection in algae. *Photosynth Res* **106**: 103-122.

Goss, R., Pinto, E.A., Wilhelm, C., and Richter, M. (2006) The importance of a highly active and delta pH-regulated diatoxanthin epoxidase for the regulation of the PSII antenna function in diadinoxanthin cycle containing algae. *J Plant Physiol* **163**: 1008-1021.

Grant, J. (1986) Sensitivity of benthic community respiration and primary production to changes in temperature and light. *Mar Biol* **90**: 299-306.

Guarini, J.M., Blanchard, G.F., and Richard, P. (2006) Modelling the dynamic of the microphytobenthic biomass and primary production in European intertidal mudflats. In *Functioning of microphytobenthos in estuaries*. Kromkamp, J.C., de Brouwer, J.F.C., Blanchard, G.F., Forster, R.M., and Créach, V. (eds). Amsterdam, the Netherlands: KNAW, pp. 187-226.

Guarini, J.M., Blanchard, G.F., Gros, P., and Harrison, S.J. (1997) Modelling the mud surface temperature on intertidal flats to investigate the spatio-temporal dynamics of the benthic microalgal photosynthetic capacity. *Mar Ecol Prog Ser* **153**: 25-36.

Hancke, K., and Glud, R.N. (2004) Temperature effects on respiration and photosynthesis in three diatom-dominated benthic communities. *Aquat Microb Ecol* **37**: 265-281.

Hancke, K., Sorell, B.K., Chresten, L., Lund-Hansen, L.C., Larsen, M., Hancke, T., and Glud, R.N. (2014) Effects of temperature and irradiance on a benthic microalgal community: A combined two-dimensional oxygen and fluorescence imaging approach. *Limnol. Oceanogr*. **59**: 1599–1611.

Haubois, A.G., Sylvestre, F., Guarini, J.M., Richard, P., and Blanchard, G.F. (2005) Spatio-temporal structure of the epipelic diatom assemblage from an intertidal mudflat in Marennes-Oleron Bay, France. *Estuar Coast Shelf S* **64**: 385-394.

Hicks, N. Bulling, M.T., Solan, M., Raffaelli, D., White, P.C.L., and Paterson, D.M. (2011) Impact of biodiversity-climate futures on primary production and metabolism in a model benthic estuarine system. *BMC Ecology*. **11**: 7.

Hynninen, P.H., Kaartinen, V., and Kolehmainen, E. (2010) Horseradish peroxidase-catalyzed oxidation of chlorophyll a with hydrogen peroxide Characterization of the products and mechanism of the reaction. *BBA-Bioenergetics* **1797**: 531-542.

Hwang, Y.-S., Jung, G., and Jin, E. (2008) Transcriptome analysis of acclimatory responses to thermal stress in Antarctic algae. *Biochem Bioph Res Co* **367**: 635-641

Ihaka, R., and Gentleman, R. (1996) R: a language for data analysis and graphics. *J Comput Graph Stat* **5**: 299-314.

Jeffrey, S.W., and Humphrey, G.F. (1975) New spectrophotometric equations for determining chlorophylls a, b c1 and c2 in higher-plants, algae and natural phytoplankton. *Biochem Physiol Pfl* **167**: 191-194.

Jesus, B., Brotas, V., Ribeiro, L., Mendes, C.R., Cartaxana, P., and Paterson, D.M. (2009) Adaptations of microphytobenthos assemblages to sediment type and tidal position. *Cont Shelf Res* **29**: 1624-1634.

Kazemipour, F., Launeau, P., and Meleder, V. (2012) Microphytobenthos biomass mapping using the optical model of diatom biofilms: Application to hyperspectral images of Bourgneuf Bay. *Remote Sens Environ* **127**: 1-13.

Kromkamp, J., Barranguet, C., and Peene, J. (1998) Determination of microphytobenthos PSII quantum efficiency and photosynthetic activity by means of variable chlorophyll fluorescence. *Mar Ecol Prog Ser* **162**: 45-55.

Kwon, T., and Watts, B.M. (1964) Malonaldehyde in aqueous solution and its role as measure of lipid oxidation in foods. *J Food Sci* **29**: 294-302.

Lavaud, J., and Lepetit, B. (2013) An explanation for the inter-species variability of the photoprotective non-photochemical chlorophyll fluorescence quenching in diatoms. *BBA-Bioenergetics* **1827**: 294-302.

Lavaud, J., and Goss, R. (2014) The peculiar features of non-photochemical fluorescence quenching in diatoms and macrophytic brown algae. In *Non-Photochemical Fluorescence Quenching and Energy Dissipation In Plants, Algae and Cyanobacteria*. Demmig-Adams, B., Garab, G., Adams, W.W.III, and Govindjee (eds). Advances in Photosynthesis and Respiration, Volume 40, pp 421-443. Dordretch, The Netherlands: Springer.

Lavaud, J., Materna, A.C., Sturm, S., Vugrinec, S., and Kroth, P.G. (2012) Silencing of the violaxanthin de-epoxidase gene in the diatom *Phaeodactylum tricornutum* reduces diatoxanthin synthesis and non-photochemical quenching. *Plos One* **7**: e36806.

Laviale, M., Ezequiel, J., Pais, C., Cartaxana P. and Serôdio, J. (submitted) A new high-resolution method for the fast vertical sampling of intertidal fine sediments.

Lefebvre, S., Mouget, J.L., and Lavaud, J. (2011) Duration of rapid light curves for determining the photosynthetic activity of microphytobenthos biofilm in situ. *Aquat Bot* **95**: 1-8.

Lepetit, B., Volke, D., Gilbert, M., Wilhelm, C., and Goss, R. (2010) Evidence for the

existence of one antenna-associated, lipid-dissolved and two protein-bound pools of diadinoxanthin cycle pigments in diatoms. *Plant Physiol* **154**: 1905-1920.

Lepetit, B., Goss, R., Jakob, T., and Wilhelm, C. (2012) Molecular dynamics of the diatom thylakoid membrane under different light conditions. *Photosynth Res* **111**: 245-257.

Lepetit, B., Sturm, S., Rogato, A., Gruber, A., Sachse, M., Falciatore, A., Kroth, P.G., and Lavaud, J. (2013) High light Acclimation in the secondary plastids containing diatom *Phaeodactylum tricornutum* is triggered by the redox state of the plastoquinone pool. *Plant Physiol* **161**: 853-865.

Lillebo, A.I., Valega, M., Otero, M., Pardal, M.A., Pereira, E., and Duarte, A.C. (2010) Daily and inter-tidal variations of Fe, Mn and Hg in the water column of a contaminated salt marsh: Halophytes effect. *Estuar Coast Shelf S* **88**: 91-98.

Mathur, S., Agrawal, D., and Jajoo, A. (2014) Photosynthesis: Response to high temperature stress. *J Photoch Photobio B* **137**: 116-126

Méléder, V., Rincé, Y., Barillé, L., Gaudin, P., and Rosa, P. (2007) Spatiotemporal changes in microphytobenthos assemblages in a macrotidal flat (Bourgneuf bay, France). *J Phycol* **43**: 1177-1190.

Méléder, V., Launeau, P., Barillé, L., Combe, J.-P. , Carrère V., Jesus, B., and Verpoorter, C. (2010) Hyperspectral imaging for mapping microphytobenthos in coastal areas. In: *Geomatic solutions for coastal environments*. Maanan, M., and Robin, M. (eds). Nova Science Publishers.

Morris, E.P., and Kromkamp, J.C. (2003) Influence of temperature on the relationship between oxygen- and fluorescence-based estimates of photosynthetic parameters in a marine benthic diatom (*Cylindrotheca closterium*). *Eur J Phycol* **38**: 133-142.

Paterson, D.M., and Hagerthey, S.E. (2001) Microphytobenthos in contrasting coastal ecosystems: Biology and dynamics. In *Ecological Comparison of Sedimentary Shores*.

Reise, K. (ed). Berlin Heildelberg: Springer-Verlag, pp. 105-125.

Perkins, R.G., Lavaud, J., Serôdio, J., Mouget, J.L., Cartaxana, P., Rosa, P. et al. (2010) Vertical cell movement is a primary response of intertidal benthic biofilms to increasing light dose. *Mar Ecol Prog Ser* **416**: 93-103.

Pinheiro, J.C., and Bates, D.M. (2000) *Mixed-models in S and S-PLUS*. New York, USA: Springer-Verlag.

Ribeiro, L., Brotas, V., Rince, Y., and Jesus, B. (2013) Structure and diversity of intertidal benthic diatom assemblages in contrasting shores: A case study from the Tagus estuary. *J Phycol* **49**: 258-270.

Rijstenbil, J.W. (2005) UV- and salinity-induced oxidative effects in the marine diatom *Cylindrotheca closterium* during simulated emersion. *Mar Biol* **147**: 1063-1073.

Roncarati, F., Rijstenbil, J.W., and Pistocchi, R. (2008) Photosynthetic performance, oxidative damage and antioxidants in *Cylindrotheca closterium* in response to high irradiance, UVB radiation and salinity. *Mar Biol* **153**: 965-973.

Saburova, M.A., and Polikarpov, I.G. (2003) Diatom activity within soft sediments: behavioural and physiological processes. *Mar Ecol Prog Ser* **251**: 115-126.

Salleh, S., and McMinn, A. (2011) The effects of temperature on the photosynthetic parameters and recovery of two temperate benthic microalgae, *Amphora cf. coffeaeformis* and *Cocconeis* cf. *sublittoralis* (Bacillariophyceae). *J Phycol* **47**: 1413-1424.

Schär, C., Vidale P.L., Lüthi, D., Frei, C., Häberli, C., Liniger, M.A., and Appenzeller, C. (2004) The role of increasing temperature variability in European summer heatwaves. *Nature* **427**: 332-336.

Serôdio, J., and Catarino, F. (1999) Fortnightly light and temperature variability in estuarine intertidal sediments and implications for microphytobenthos primary productivity. *Aquat. Ecol.* **33**: 235-241.

Serôdio, J., Cartaxana, P., Coelho, H., and Vieira, S. (2009) Effects of chlorophyll fluorescence on the estimation of microphytobenthos biomass using spectral reflectance indices. *Remote Sens Environ* **113**: 1760-1768.

Serôdio, J., and Lavaud, J. (2011) A model for describing the light response of the nonphotochemical quenching of chlorophyll fluorescence. *Photosynth Res* **108**: 61-76.

Serôdio, J., Cruz, S., Vieira, S., and Brotas, V. (2005) Non-photochemical quenching of chlorophyll fluorescence and operation of the xanthophyll cycle in estuarine microphytobenthos. *J Exp Mar Biol Ecol* **326**: 157-169.

Serôdio, J., Ezequiel, J., Frömmlet, J., Laviale, M., and Lavaud, J. (2013) A method for the rapid generation of non-sequential light-response curves of chlorophyll fluorescence. *Plant Physiol* **163**: 1089-1102.

Serôdio, J., Ezequiel, J., Barnett, A., Mouget, J.L., Méléder, V., Laviale, M., and Lavaud, J. (2012) Efficiency of photoprotection in microphytobenthos: role of vertical migration and the xanthophyll cycle against photoinhibition. *Aquat Microb Ecol* **67**: 161-175.

Solomon, S., Qin, D., Manning, M., Chen, Z., Marquis, M., Averyt, K.B., Tignor, M., and Miller, H.L. (eds.) (2007) Contribution of Working Group I to the Fourth Assessment Report of the Intergovernmental Panel on Climate Change. In *Climate Change 2007: Impacts, Adaptation and Vulnerability.* 996 pp., Cambridge University Press, Cambridge, United Kingdom and New York, NY, USA.

Stott, P.A., Stone, D.A., and Allen, M.R. (2004) Human contribution to the European heatwave of 2003. *Nature* **432**: 610-614.

Underwood, G.J.C., and Kromkamp, J. (1999) Primary production by phytoplankton and microphytobenthos in estuaries. In *Advances in Ecological Research, Vol 29: Estuaries*, pp. 93-153.

van Leeuwe, M.A., Brotas, V., Consalvey, M., Forster, R.M., Gillespie, D., Jesus, B. et al.

(2008) Photoacclimation in microphytobenthos and the role of xanthophyll pigments. *Eur J Phycol* **43**: 123-132.

Vanelslander, B., Creach, V., Vanormelingen, P., Ernst, A., Chepurnov, V.A., Sahan, E. et al. (2009) Ecological differentation between sympatric pseudocryptic species in the estuarine benthic diatom *Navicula phyllepta* (Bacillariophyceae). *J Phycol* **45**: 1278-1289.

Vieira, S., Ribeiro, L., da Silva, J.M., and Cartaxana, P. (2013) Effects of short-term changes in sediment temperature on the photosynthesis of two intertidal microphytobenthos communities. *Estuar Coast Shelf S* **119**: 112-118.

Wang, Z.-H., Nie, X.-P., Yue, W.-J., and Li, X. (2012) Physiological responses of three marine microalgae exposed to cypermethrin. *Environ Toxicol* **27**: 563-572.

Waring, J., Klenell, M., Bechtold, U., Underwood, G.J.C., and Baker, N.R. (2010) Light-induced responses of oxygen photoreduction, reactive oxygen species production and scavenging in two diatom species. *J Phycol* **46**: 1206-1217.

Westermann, M., and Rhiel, E. (2005) Localisation of fucoxanthin chlorophyll a/c-binding polypeptides of the centric diatom *Cyclotella cryptica* by immuno-electron microscopy. *Protoplasma* **225**: 217-223.

Witkowski, A., Sullivan, M.J., Bogaczewicz-Adamczak, B., Bak, M., Rhiel, E., Ribeiro, L., and Richard, P. (2012) Morphology and distribution of a little known but widespread diatom (Bacillariophyceae), *Navicula spartinetensis* Sullivan et Reimer. *Diatom Res* **27**: 43-51.

Wu, H.Y., Roy, S., Alami, M., Green, B.R., and Campbell, D.A. (2012) Photosystem II photoinactivation, repair, and protection in marine centric diatoms. *Plant Physiol* **160**: 464-476.

Yun, M.S., Lee, S.H., and Chung, I.K. (2010) Photosynthetic activity of benthic diatoms in response to different temperatures. *J Appl Phycol* **22**: 559-562.

Zhu, S.H., and Green, B.R. (2010) Photoprotection in the diatom *Thalassiosira pseudonana*: Role of LI818-like proteins in response to high light stress. *BBA-Bioenergetics* **1797**: 1449-1457.

Figure legends

Figure 1

In situ environmental conditions and photosynthetic activity of microphytobenthos during a summer diurnal emersion in Portuguese (Ria de Aveiro, Vista Alegre, A- and C-) and French (Baie de l'Aiguillon, Esnandes, B- and D-) intertidal flats. A- and B- Photosynthetic Active Radiation (PAR, µmol photons m^{-2} s^{-1}, black line) at the surface of the sediment and temperature (°C) at five depths (surface, -0.5 cm, -2 cm, -5 cm, -10 cm, grey lines); C- and D- effective PSII quantum yield (ΦPSII: open squares) and maximum non-photochemical quenching of Chl *a* fluorescence (NPQ_{max}: closed circles). Local time (FR: UTC+1, PT: UTC).

Figure 2

Index of photoinhibition (decrease in ΦPSII) of microphytobenthos harvested at the French site (FR) during light stress recovery experiments performed on sediment exposed at two temperatures (27°C, A- or 37°C, B-) and with an inhibitor of cell motility (+ Lat A) or without (Ctrl). T_0, beginning of the experiment under low light (50 µmol photons m^{-2} s^{-1}); HL, after 3 h high light (1200 µmol photons m^{-2} s^{-1}); Recov, after 15 min recovery under low light (50 µmol photons m^{-2} s^{-1}) following the 3 h high light; LL, after 3 h of low light (50 µmol photons m^{-2} s^{-1}). Values are mean ± SD (n=6).

Figure 3

Index of photoprotection (NPQ) of microphytobenthos harvested at the French site (FR) during light stress recovery experiments performed on sediment exposed at two temperatures (27°C, A- or 37°C, B-) and with an inhibitor of cell motility (+Lat A) or without (Ctrl). Legend as in Fig. 2**.** Values are mean ± SD (n=6).

Figure 4

Pigment content makers of photooxidative stress (Chl *a* allomerization ratio: AR) and of photoprotection (DD+DT pool; DD de-epoxidation state: DES) of microphytobenthos harvested at the French site (FR) during light stress recovery experiments performed on sediment exposed at two temperatures (27°C or 37°C) and with an inhibitor of cell motility (+Lat A) or without (Ctrl). A- AR, data from 27 and 37°C experiments were pooled, * significant difference compared to Ctrl at the same time ($P < 0.05$, Tukey HSD); B- DD+DT pool (in mol.100 mol Chl a^{-1}), data from Ctrl and Lat A-treated samples were pooled, ** significant difference compared to 27 °C at the same time ($P < 0.01$, Tukey HSD); C- and D- DES, *** significant difference compared to Ctrl at the same time ($P < 0.001$, Tukey HSD). Labels as in Fig. 2. Values are mean ± SD (n=12: A,B or n=6: C,D) expressed as $\%T_0$.

Figure 5

Western blot of the Lhcx proteins of microphytobenthos harvested at the French site during light stress recovery experiments performed on sediment exposed at two temperatures (27°C, A- or 37°C, B-) and with an inhibitor of cell motility (+) or without (-). HL, after 3 h HL (1200 µmol photons m^{-2} s^{-1}); LL, after 3 h of LL (50 µmol photons m^{-2} s^{-1}). All samples were normalized to the same Chl *a* concentration (15 µg Chl *a* mL^{-1}). A-

Lhcx proteins were detected using a monoclonal anti-FCP6 (Lhcx1). This antibody detects, similarly as the anti-LHCSR of *C. reinhardtii* (Lepetit *et al.*, 2013), also Lhcx2 and Lhcx3 in *P. tricornutum* (strain 'P.t.1') used here as a control. *N. phyllepta* s.l. (N.p.), the dominant species of the MPB community, was also tested. B- and C- Lhcx proteins were detected using a monoclonal anti-Lhcx6 from *T. pseudonana* (T.p.) (Zhu and Green, 2010) which also potentially detect Lhcx3 and an Lhcx dimer in *P. tricornutum* ; C- is a special focus on the band between 33-50 kDa in 37°C exposed samples. Revelation times were: A- 30 s; B- 15 s for the bands between 17-23 kDa, 45 s for the band between 33-50 kDa; C- 30 s;. Note that for A- all samples exposed at 37°C did not yield satisfying signal; and for B-, the sample HL+ 27°C was lost.

Figure 6

Amount of lipid peroxidation marker (TBARS content in 10^{-6} nmol MDA equivalent mL^{-1}) in microphytobenthos harvested at the French site (FR) during light stress recovery experiments performed on sediment exposed at two temperatures (27°C, A- or 37°C, B-) with an inhibitor of cell motility (+Lat A). Labels as in Fig. 2. Values are mean ± SD (n=6) normalized to surface biomass (I_{diat} biomass index).

Figure 7

Comparison of photoinhibition level (decrease in ΦPSII) and photoprotection (NPQ) in microphytobenthos harvested at the Portuguese (PT) and the French (FR) sites during light stress recovery experiments performed on sediment exposed at two temperatures (27°C or 37°C) and with an inhibitor of cell motility (+Lat A) or without (Ctrl). ΦPSII

recovery (A) and sustained NPQ (B) after 15 min incubation under LL (50 µmol photons m^{-2} s^{-1}) following 3 h of HL exposure (1200 µmol photons m^{-2} s^{-1}), *** significant difference between sites ($P < 0.001$, Tukey HSD). Values are mean ± SD (n=6).

Figure 8

Western-blot of the Lhcx proteins of microphytobenthos harvested at the Portuguese site during light stress recovery experiments performed on sediment exposed at two temperatures (27°C or 37°C) and with an inhibitor of cell motility (+) or without (-). HL, after 3 h HL (1200 µmol photons. m^{-2}. s^{-1}) treatment; LL, after 3 h of LL exposure. All samples were normalized to the same Chl *a* concentration (15 µg Chl *a* mL^{-1}). Lhcx proteins were detected using a monoclonal anti-FCP6 (Lhcx1). This antibody detects, similarly as the anti-LHCSR of *C. reinhardtii* (Lepetit *et al.*, 2013), also Lhcx2 and Lhcx3 in *P. tricornutum* (strain 'P.t.1') used here as a control. Note that i) the 27°C and 37°C samples were not loaded on the same gel but the revelation time was the same (30 s), ii) the use of the monoclonal anti-Lhcx6 from *T. pseudonana* did not yield any signal with these samples.

Figure 1_Laviale *et al.*

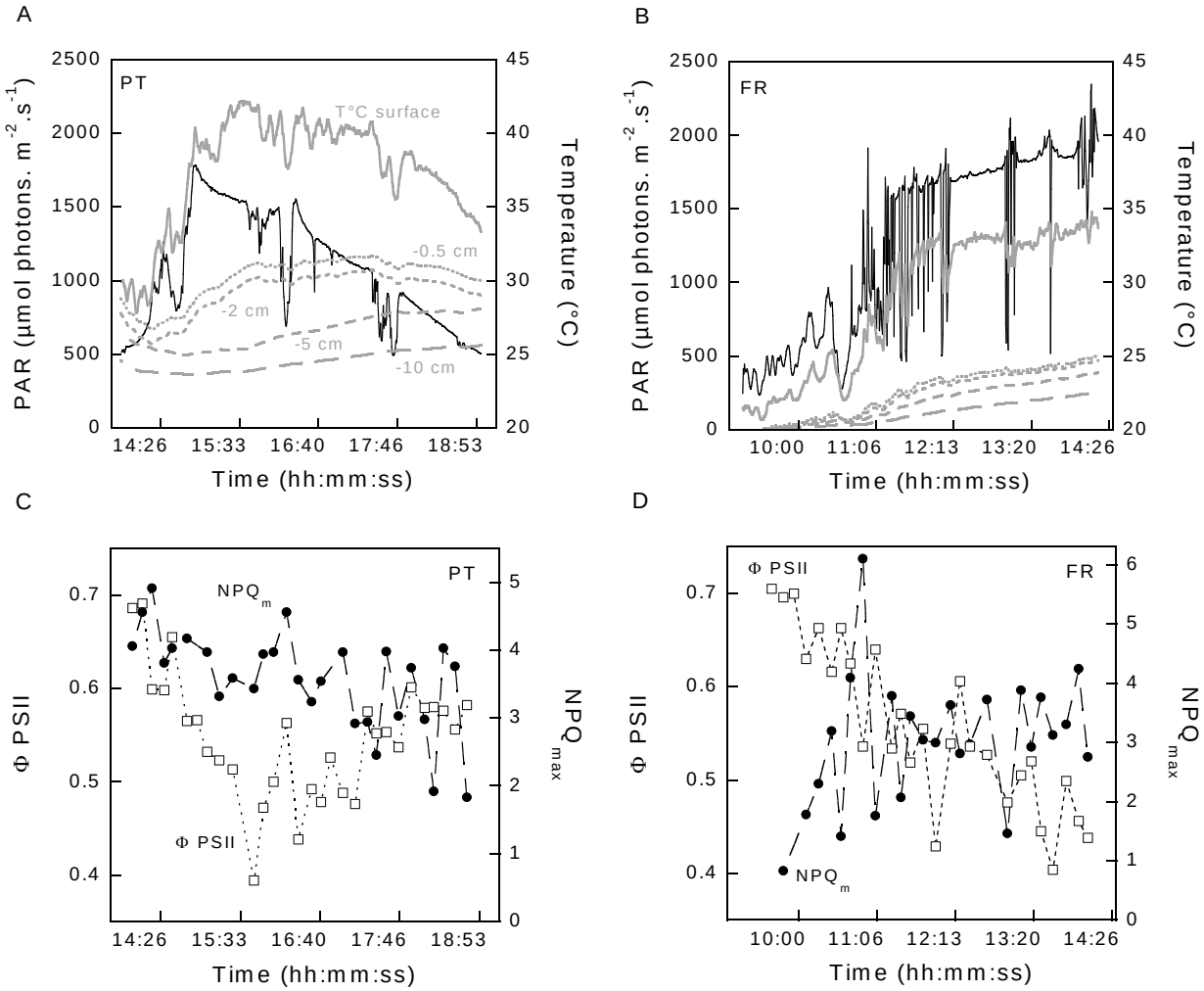

Figure 2_Laviale *et al.*

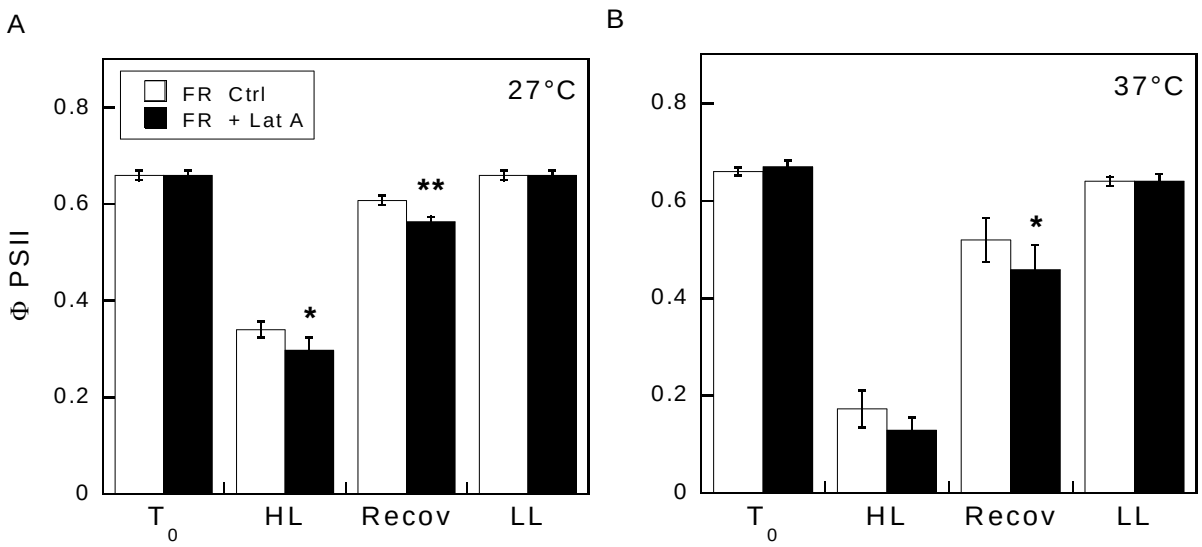

Figure 3_Laviale *et al.*

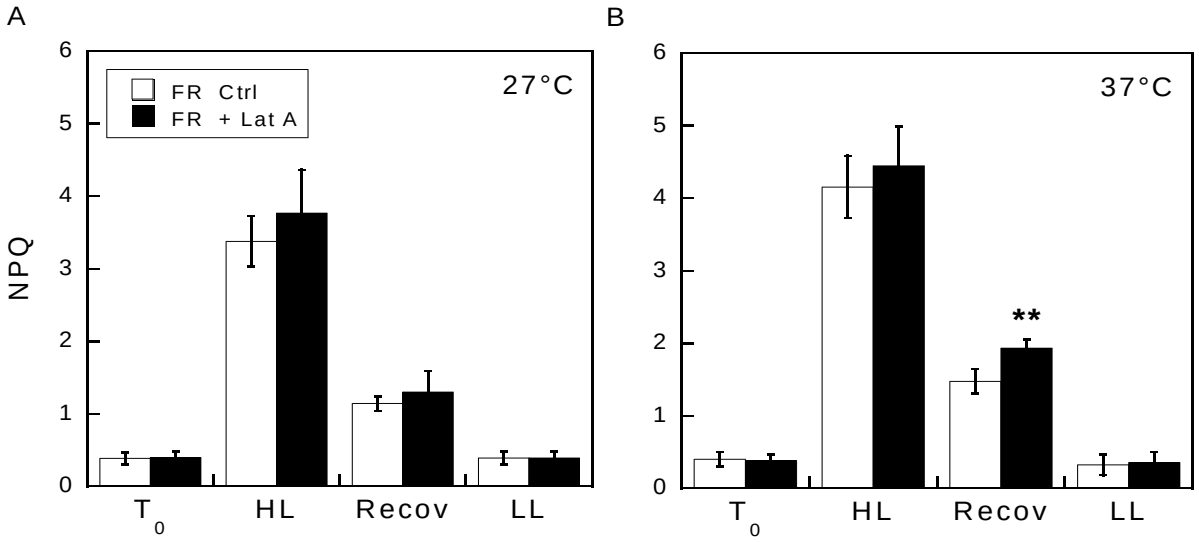

Figure 4_Laviale *et al.*

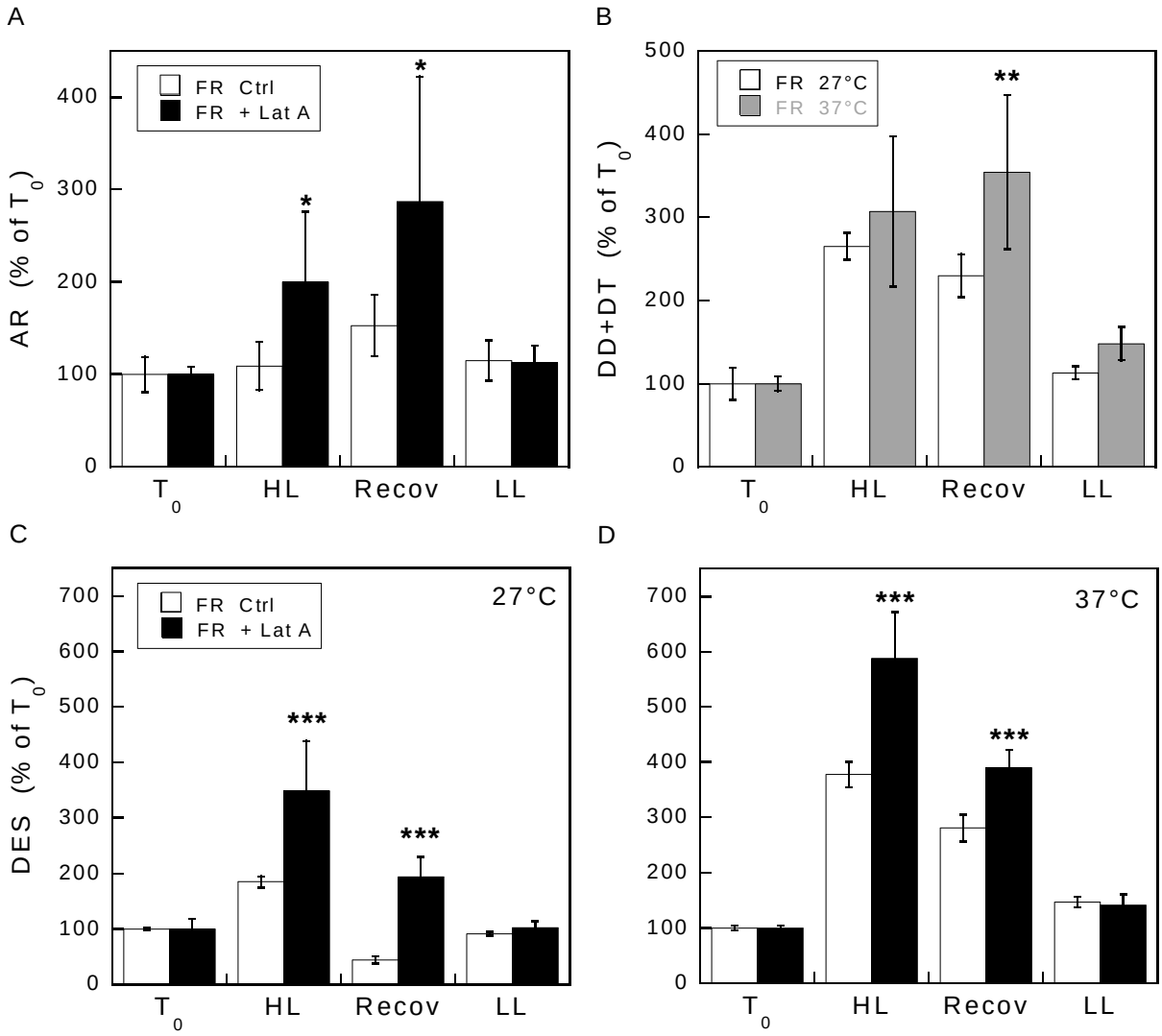

Figure 5_Laviale *et al.*

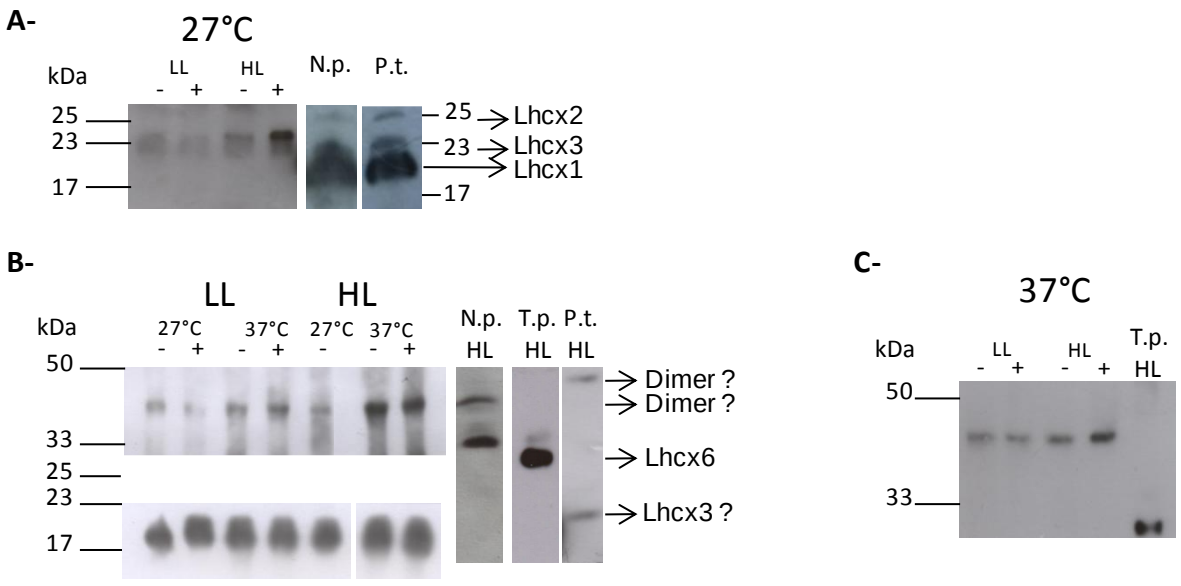

Figure 6_Laviale *et al.*

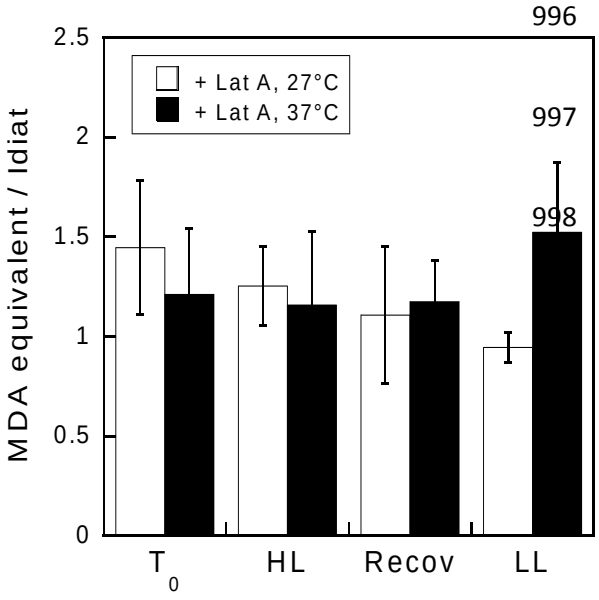

Figure 7_Laviale *et al.*

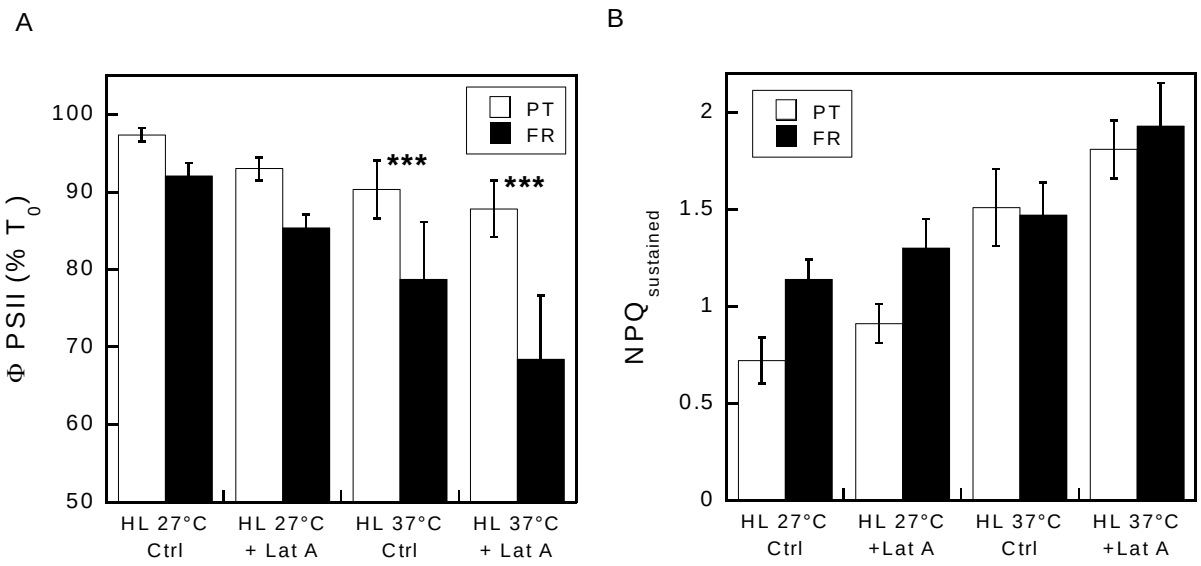
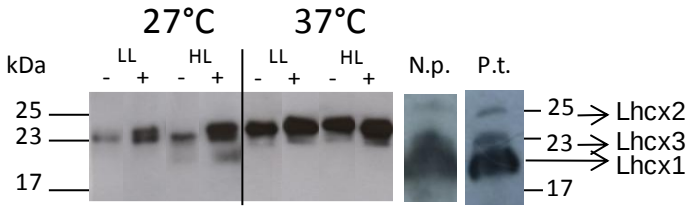
Figure 8_Laviale *et al.*